

# Feature Length-Scale Modeling of LPCVD & PECVD MEMS Fabrication Processes

LAWRENCE C. MUSSON, <sup>+</sup>PAULINE HO, STEVEN J. PLIMPTON, RODNEY C. SCHMIDT

*Sandia National Laboratories*

*P.O. Box 5800 MS 0316*

*Albuquerque, NM USA 87185*

<sup>+</sup>*Reaction Design, Inc.*

*6440 Lusk Blvd. Suite D2009*

*San Diego, CA USA 92121*

The surface micromachining processes used to manufacture MEMS devices and integrated circuits transpire at such small length scales and are sufficiently complex that a theoretical analysis of them is particularly inviting. Under development at Sandia National Laboratories (SNL) is Chemically Induced Surface Evolution with Level Sets (ChISELS), a level-set based feature-scale modeler of such processes. The theoretical models used, a description of the software and some example results are presented here. The focus to date has been of low-pressure and plasma enhanced chemical vapor deposition (LPCVD & PECVD) processes. Both are employed in SNL's SUMMiT V technology. Examples of step coverage of SiO<sub>2</sub> into a trench by each of the LPCVD and PECVD process are presented.

*Keywords:* MEMS, CVD, LPCVD, PECVD, level-set method, feature scale.

## 1. Introduction

In the surface micromachining (SMM) approach to the fabrication of MEMS devices three-dimensional (3D) structures are formed by deposition and etching of thin films. Careful construction of the lithographic masks that control these steps and the application of a final selective release etch permits the creation of a variety of free-standing movable parts. SMM fabrication can involve a wide variety of chemical processes in the deposition and etching steps. For example, deposition processes in the SUMMiT V (Rodgers and Sniegowski 1998)

technology developed by Sandia National Labs include low-pressure chemical vapor deposition (LPCVD) of undoped polysilicon, P-doped polysilicon, silicon dioxide from TEOS  $[\text{Si}(\text{C}_2\text{H}_5\text{O})_4]$ , and Si-rich silicon nitride from  $\text{SiCl}_2\text{H}_2$  and  $\text{NH}_3$ , as well as steam oxidation for the initial  $\text{SiO}_2$  layer and the plasma deposition (PECVD) of  $\text{SiO}_2$  from  $\text{SiH}_4$  and  $\text{O}_2$ . Etching processes include a plasma etch of oxide and nitride using  $\text{C}_2\text{F}_6$  and  $\text{CHF}_3$ , of polysilicon using  $\text{Cl}_2$ , He, and/or HBr, and a wet etch using aqueous HF.

Many of the above mentioned deposition and etching processes can result in non-ideal device geometries at the feature scale. For example, CVD processes give near-conformal films, which yield rounded corners and dimples. Step coverage can range from perfectly conformal to non-conformal, and lower step coverage can result in sloped sidewalls. Under some conditions non-uniformities and irregularities in surface coverage occur. The unexpected appearance of any of these types of geometric irregularities can be particularly costly in the design, analysis, and batch fabrication cycle associated with the development of a new MEMS device. Thus a thorough understanding of the detailed chemistry and physics which lead to these geometric variations is essential to the development of improved SMM fabrication equipment, higher yield and more reliable fabrication processes, and more useful MEMS designs.

## **2. Theoretical Modeling at the Feature Scale with ChISELS**

Theoretical modeling of the detailed surface chemistry and concomitant surface evolutions during microsystems fabrication processes misrecognized as having a great potential for improving SMM process fabrication technologies. The viability of computational simulations for these types of problems has been clearly demonstrated by earlier researchers and advances have been made in developing transport models, chemical mechanisms, and surface evolution modeling, *e.g.* see Cale, *et al.* (2000) and Sethian (1996). However, currently available computer codes have not been designed to use massively parallel architectures efficiently, nor to exploit all of the modeling advances that different researchers have made. Thus speed and robustness factors have unduly limited the size and complexity of problems that can be treated with available tools.

To overcome these limitations, we are developing a computer code called ChISELS (Chemically Induced Surface Evolution with Level-Sets), a parallel, 2D and 3D feature-scale modeler to explore the time development of material deposition/etch on patterned wafers at low pressures. ChISELS is a platform to build and improve on previous simulation tools while taking advantage of the most recent advances in dynamic mesh refinement, load balancing, and highly scalable solution algorithms.

There are three inter-related aspects to modeling the overall physics of the problem: (1) transport of chemical species, (2) gas phase and surface chemistry, and (3) the dynamic evolution of the solid surface.

Currently, all gas-phase transport is assumed to occur in the free-molecular flow regime (i.e., particle-particle collisions are negligible). In ChISELS, we adopt the ballistic transport and reaction model (BTRM) developed and described by Cale and coworkers (Cale et al. 2000; Cale and Mahadev 1996). An important aspect of this method is the need to calculate view-factors for each surface element of the discretized feature surface. Chaparral (Glass 2001), a radiation heat transfer modeler, is used for this purpose. The flux of species  $k$  to surface element  $i$  is computed from

$$F_{ik} = F_{ik}^0 + G_{ij}(F_{jk} + R_{jk}) \quad 1$$

where  $F_{ik}^0$  is the direct flux from the bulk of the reactor,  $G_{ij}$  is the view factor between surface  $i$  and  $j$ ,  $F_{jk}$  is the flux of species  $k$  to surface  $j$ ,  $R_{jk}$  is the reaction rate of species  $k$  on surface  $j$ , and, by Einstein's convention, repeated indices in the product imply summation.

Deposition or etching occurs through the chemical reaction of gas phase species with bulk and surface phase species at the feature surface. The thermodynamics and heterogeneous surface chemistry of these reactions are modeled in ChISELS by coupling with Surface Chemkin®. This requires the specification of a chemical reaction mechanism for each surface reaction to be modeled in the simulation.

Feature scale microsystem fabrication modelers such as ChISELS are at heart topology modelers, *i.e.* they model the evolution of a free boundary according to the physics that cause it to move. Chisels uses an implicit surface-tracking approach called the level-set method (Sethian 1996). In the level-set method, a domain-spanning function,  $\phi$  is defined; the zero-value contour, or level set, of which conforms to the feature surface. The level-set function is evolved by solving the scalar partial-differential equation,

$$\frac{\partial \phi}{\partial t} + \mathbf{v} \cdot \nabla \phi = 0 \quad 2$$

over the volume and integrating through time. The velocity,  $\mathbf{v}$ , is called the extension velocity and is defined over the entire domain. The extension velocity must be chosen so that the level set of  $\phi$  evolves in such a way that it represents the evolution of the feature surface; *i.e.* it is chosen based on the velocity of the surface--the deposition or etch rate. The level set method avoids the debilitations of explicit conform-and-track methods because the mesh which is used to solve Equation 2 does not deform, so distortion effects are avoided. Likewise, because a volume-defined function is evolved, merging surfaces do not create problems in the method. Equation 2 is solved by an augmented method of characteristics (Strain 2000).

Additional details of the methods and models that ChISELS uses can be found in Musson *et al.* (2003) or on the ChISELS web site, <http://www.cs.sandia.gov/~wchisels>.

### 3. Examples

A three-dimensional and two two-dimensional examples are provided here of ChISELS results. The three-dimensional example is of the deposition of polysilicon into a hub shape. Of the two-dimensional examples, the first is of the deposition of SiO<sub>2</sub> into a 10x1 trench using silane by a PECVD process. The other is the deposition of SiO<sub>2</sub> into an identical trench using TEOS. In each case, the deposition rate as a function of depth in the trench is presented.

In none of the three cases has the chemistry mechanisms used been validated at the feature scale. The data produced and presented, however, still serves as a useful exhibition of the capabilities of the ChISELS software. Indeed, one of the designed uses of this software is to aid chemists in refining chemistry mechanisms at these length scales.

### 3.1 LPCVD of Poly-Si from SiH<sub>4</sub>

An example of the deposition of polysilicon onto the three-dimensional surface depicted in Figure 1 illustrates the 3D modeling capability of ChISELS and why first principles modeling is important. The chemistry mechanism employed in this example is simplified from the one published in Ho *et al.* (1994).

The gas composition in the reactor immediately above the wafer surface is a required input to ChISELS. Because that composition is unlikely to be identical to that introduced into the reactor, a reactor-scale model must be employed to provide the mole fractions of the introduced reactants and their products near the wafer. In this simple test case, however, the reactor compositions were simply set to somewhat arbitrary values.

Figure 2 shows the surface after a time period of deposition of polysilicon onto the surface. In this case, the reactor composition, a required input to ChISELS, is 100% mol SiH<sub>4</sub>. The step coverage is quite uniform because of the low reactivity of silane. Notice the small voids that form when the inside portion of the feature closes up. ChISELS is able to model such events without user interaction and is the primary reason why the level-set method is our choice for modeling the evolving interfaces in these kinds of problems.

When the reactor composition is changed slightly, there is a dramatic change in the final surface shape. Figure 3 shows the surface after deposition when the reactor composition is 99.9 % mol SiH<sub>4</sub> and 0.1 % mol SiH<sub>2</sub>. The high reactivity of the SiH<sub>2</sub> causes the non-uniform deposition seen in the figure. These non-conformal depositions, whether not-nearly conformal or only slightly so, are the

reasons why it can be advantageous to model the process steps alongside design or in process development.

### 3.2 PECVD of SiO<sub>2</sub> from Ar, O<sub>2</sub>, SiH<sub>4</sub>

The deposition of silicon dioxide into a trench of aspect ratio 10:1 (*cf.* Figure 4) from a mixture of SiH<sub>4</sub>, O<sub>2</sub>, Ar and derivative compounds in a high-density plasma reactor is modeled by ChISELS. The grid used to model the process is also shown in Figure 4.

The chemistry mechanism used in this model is the one published by Meeks *et al.* (1998). This is a system with 46 gas-phase species, 13 surface-phase species and 205 surface reactions.

As before, the reactor gas-phase composition must be specified. In this case, Aurora, a zero-D reactor-scale modeler and Reaction Design product, part of the Chemkin suite, was used to determine those compositions. The inlet conditions provided to Aurora are a temperature of 300K, and mole fractions of 0.0097, 0.0223 and 0.9680 respectively of SiH<sub>4</sub>, O<sub>2</sub> and Ar at a total flow rate of 0.0028 g/s. The output of Aurora is the mole fractions of all reactants and products at the wafer as well as surface, ion and electron temperatures and ion energy. All of these are inputs to ChISELS.

Figure 5 shows the deposition rate in the trench as a function of its depth for the indicated pressures of 0.03, 0.04 and 0.05 Torr. As shown in the figure and perhaps contrary to intuition, the lowest pressure of 0.03 Torr actually produced the highest growth rate of all pressures tried. This is due to the difference in the gas-phase composition at the reactor due to a change of reactor pressure. This underscores the importance of coupling ChISELS to a reactor-scale model.

As Figure 5 shows, the deposition rate, and thus step coverage, in this process is not uniform. The deposition rate at about 75% depth of the trench is about two orders of magnitude smaller than at the top. The source of the non-uniformity is

most likely due to the plasma forming highly reactive radicals that get depleted almost entirely near the top of the trench and are hardly present near the bottom. Note that the deposition rate increases again near the bottom of the trench. This is due to the presence of ion-enhanced reactions. The nearly collimated flow of ions affect the sidewalls only slightly because the flow is nearly parallel to them. Near the bottom, the greater ion bombardment changes the ratio of surface site species that changes the ratio of the reactions that produce deposition. Note also that there are some higher growth rates on the ordinate of Figure 5. These points correspond to surface elements near the center of the bottom plane of the trench. These higher growth rates are owed to greater visibility of the reactor and its neutral radical constituents above as well as a greater incident flux of ions.

Figure 6 shows the deposition rate in the trench as a function of depth and bias power on the wafer as reflected by the ion energy. The pressure in each of the three cases is fixed at 0.03 Torr and the ion energies used were 15 eV, 40 eV and 60 eV. The deposition rates in each case are similar, as expected, where the ions are least influential. Near the mouth of the trench, there is some increase in deposition rate owing to the change in surface site species due to ion-enhanced reactions. The same can be said of the deposition rates near the bottom of the trench, though there is one other factor at work there.

Whereas in the case of the lowest ion energy, the deposition rates on the bottom surface of the trench are higher, as previously explained, than those on the adjacent sidewalls, the deposition rates on the bottom surface for each of the other two ion energies is lower than the rates on the adjacent sidewalls. This is because, in the former, the ion energy of 15 eV is lower than the threshold of 35 eV at which sputtering begins. The only action of the ions in this case is to change site types. In the cases of the two higher ion energies, there is some sputtering of  $\text{SiO}_2$  on the bottom surface; thus the net deposition rate is reduced. In fact, in the 60 eV ion energy case, there is a net removal of material from the bottom. The  $\text{SiO}_2$  that is sputtered off the bottom is redeposited on the sidewalls near the bottom of the trench. This effect, in addition to the ion-enhanced reactions, is why the deposition rate on the sidewalls is increased and the bottom rate is decreased for ion energies above the sputtering threshold.

### 3.3 LPCVD of SiO<sub>2</sub> from TEOS

The second example is the deposition of SiO<sub>2</sub> into a trench from TEOS. The trench geometry and grid are identical to the first example. There are two chemistry mechanisms used in this example. The first is a mechanism published by Coltrin *et al.* (2000), and the second by IslamRaja *et al.* (1993). Once again, Aurora is used to compute gas-phase composition. The mechanism used in Aurora is Coltrin's. The IslamRaja mechanism is defined only for heterogeneous reactions. The input conditions are a reactor temperature of 1003K--the temperature at which the IslamRaja mechanism was tuned and the only temperature for which it is truly valid--pressures of 0.3, 0.4 and 0.5 Torr and an inlet flow rate of 0.046 g/s of TEOS and N<sub>2</sub> with mole fractions of 0.13 and 0.87 respectively.

Figures 7 and 8 show the deposition rate of SiO<sub>2</sub> as a function of the depth in the trench. Unlike the previous example, the deposition rate as predicted by both mechanisms increases with the reactor pressure. The difference between the two TEOS mechanisms is the magnitude and uniformity of the deposition rate. Coltrin's mechanism predicts a lower overall rate and one which is exceptionally uniform. The IslamRaja mechanism produces a very non-uniform deposition rate varying two orders of magnitude from the bottom of the trench to the top.

Experiments have shown the deposition of SiO<sub>2</sub> indeed to be non-uniform. So Coltrin's mechanism clearly does not work at the feature scale though it has been shown to work on the reactor scale. The IslamRaja mechanism is not even defined on the reactor scale, so there is no way to couple ChISELS to a reactor-scale model with that mechanism in use. The next step is to refine Coltrin's mechanism so that it remains working on the reactor scale and also produces realistic growth rates at the feature scale.



## 4. Summary

A cursory description of the ChISELS feature length-scale modeler has been given. Examples were discussed of the deposition polysilicon into a 3D feature by silane, of SiO<sub>2</sub> by LPCVD through TEOS and by PECVD through silane and oxygen in plasma in 2D features. Step coverages for each process and how they are affected by reactor operating conditions were shown. More details of the Chisels software can be found in Musson *et al.* (2003) and <http://www.cs.sandia.gov/~wchisels>.

## 5. Acknowledgements

The authors would like to thank Sandia National Laboratories and the U.S. Department of Energy for supporting this work. Sandia is a multiprogram laboratory operated by Sandia Corporation, a Lockheed-Martin company, for the United States Department of Energy under Contract DE-AC04-94AL85000.

## 6. References

- M. S. Rodgers, J. J. Sniegowski, "Designing Microelectromechanical Systems-on-a-Chip in a 5-Level Surface Micromachine Technology," 2nd Int. Conf. Eng. Design and Automation, 1998.
- T. S. Cale, T. P. Merchant, L. J. Borucki and A. H. Labun, Thin Solid Films, 356, 152-175, 2000.
- A. H. Labun, H. K. Moffat and T. S. Cale, J. Vac. Sci. Technol. B., 18, 267-278.
- J. A. Sethian, "Level Set Methods", Cambridge Univ. Press, Cambridge, 1996.
- T. S. Cale and V. Mahadev, in Thin Films: Modeling of Film Deposition for Microelectronic Applications, Vol. 22, Ed. S. Rosnagel, Academic Press, 176-277, 1996.
- M. W. Glass, "{CHAPARRAL}": A library for solving enclosure radiation heat transfer problems", Sandia National Laboratories, Albuquerque, NM, 2001.
- J. Strain, J. Comput. Phys., 161, 512--528, 2000.

Musson, Lawrence C., Plimpton, Steven J., and Schmidt, Rodney C. MEMS Fabrication Modeling with ChISELS: A Massively Parallel 3D Level-Set Based Feature Scale modeler, Technical Proceedings of the 2003 Nanotechnology Conference and Trade Show, Volume 3 Nanotech 2003 Grand Hyatt San Francisco, San Francisco, CA, U.S.A. February 23-27, 2003

Ellen Meeks, Richard Larson, Pauline Ho, Christopher Apblett, Sang M. Han, Erik Edelberg and Eray S. Aydil, J. Vac. Sci. Technol. A, 16(20), 544--563, 1998.

Michael E. Coltrin, Pauline Ho, Harry K. Moffat and Richard J. Buss, Thin Solid Films, 365, 251--263, 2000.

M. M. IslamRaja, C. Chang, J. P. McVittie, M. A. Cappelli and S. C. Saraswat, J. Vac. Technol. B 11(3), 720--726, 1993.

P. Ho, M. E. Coltrin, W. G. Breiland, "Laser-Induced Fluorescence Measurements and Kinetic Analysis of Si Atom Formation in a Rotating Disk Chemical Deposition Reactor," J. Phys. Chem. **98**, 10138, 1994.

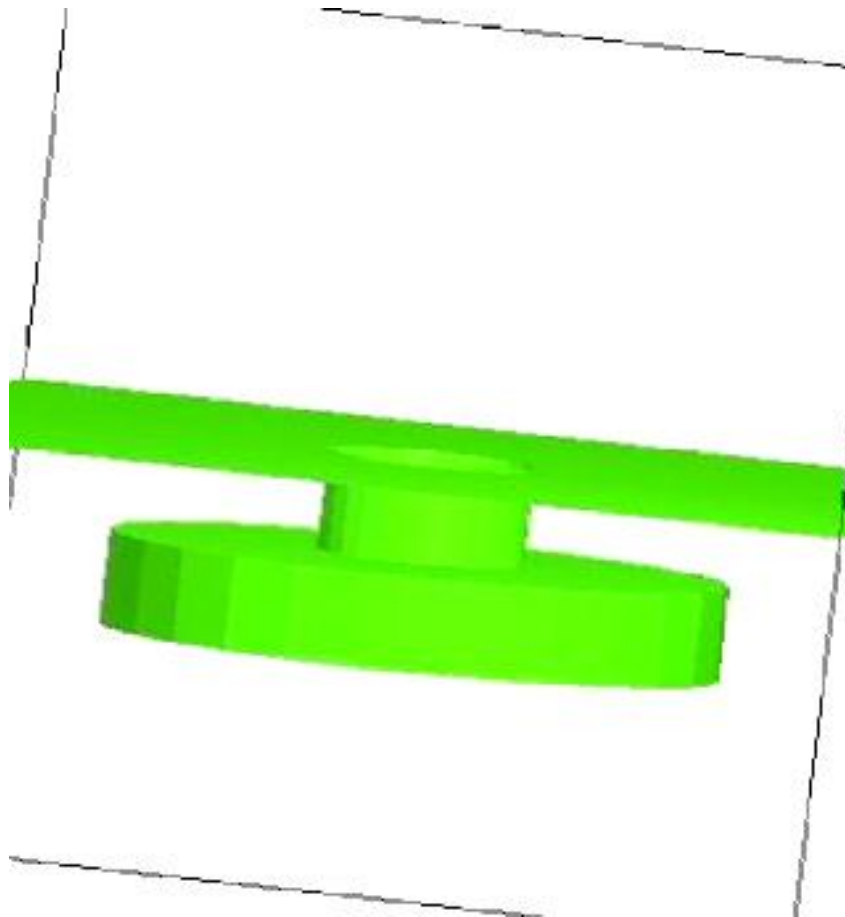


**Figure 1** Initial shape of 3D test feature. The volume below the surface is solid, above is gas.

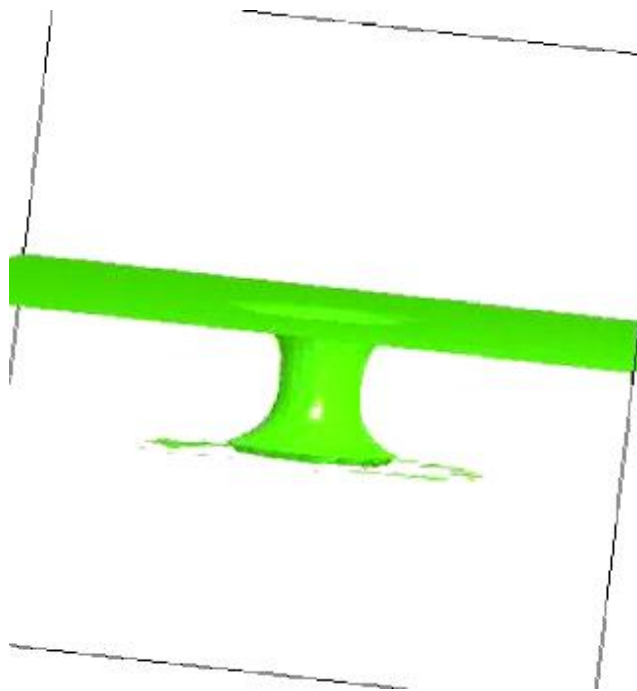


**Figure 2** Shape of the feature after deposition of polysilicon from 100%  $\text{SiH}_4$ .

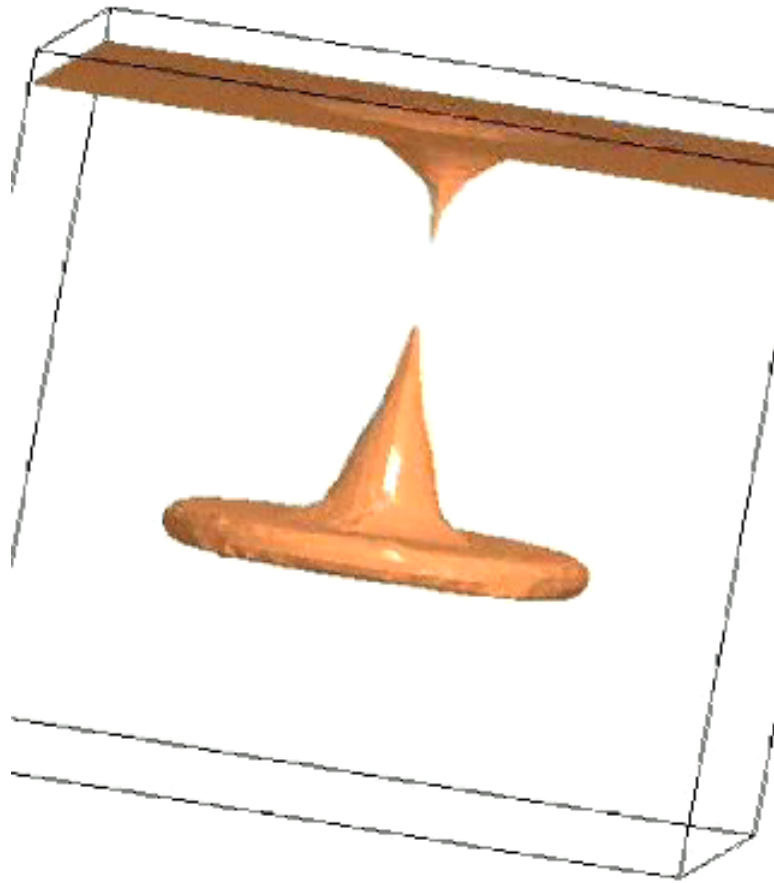


**Figure 3** Shape of the 3D feature after deposition of polysilicon from 99.9% mol  $\text{SiH}_4$  and 0.1 % mol  $\text{SiH}_2$ .

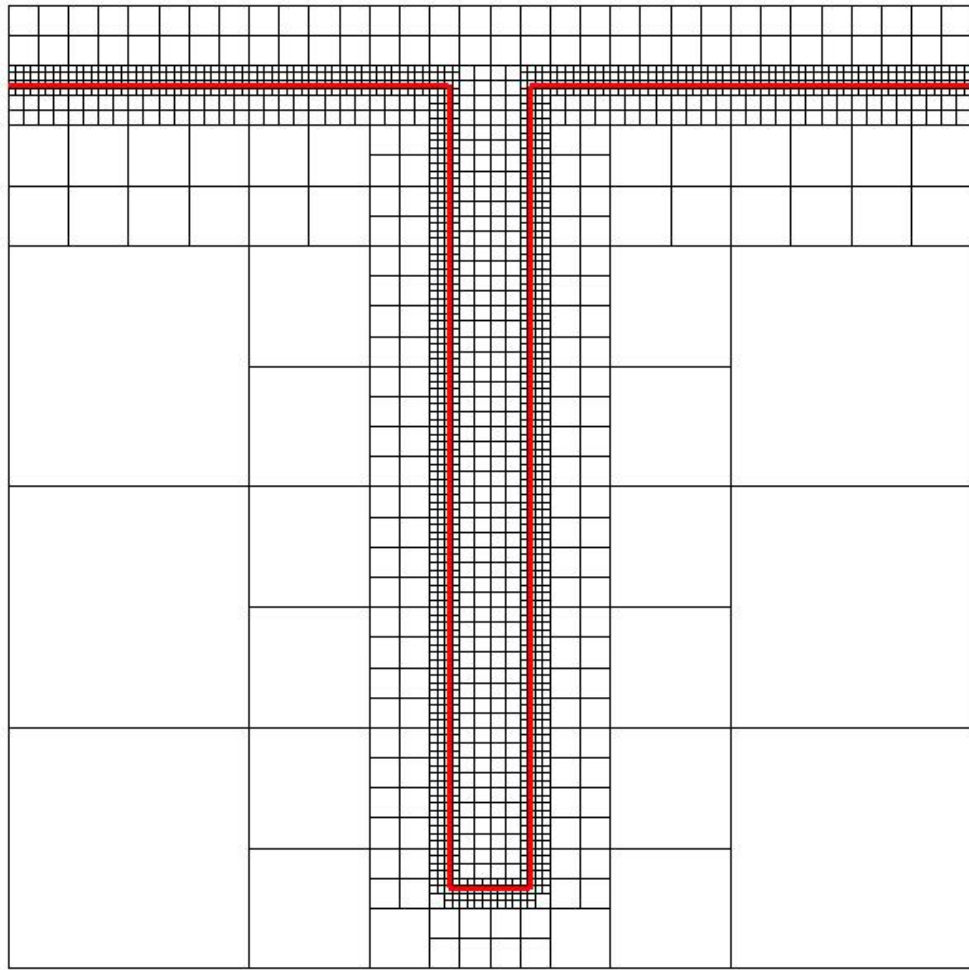


**Figure 4** Initial shape of the surface and the initial grid used in the 2D PECVD and LPCVD examples.

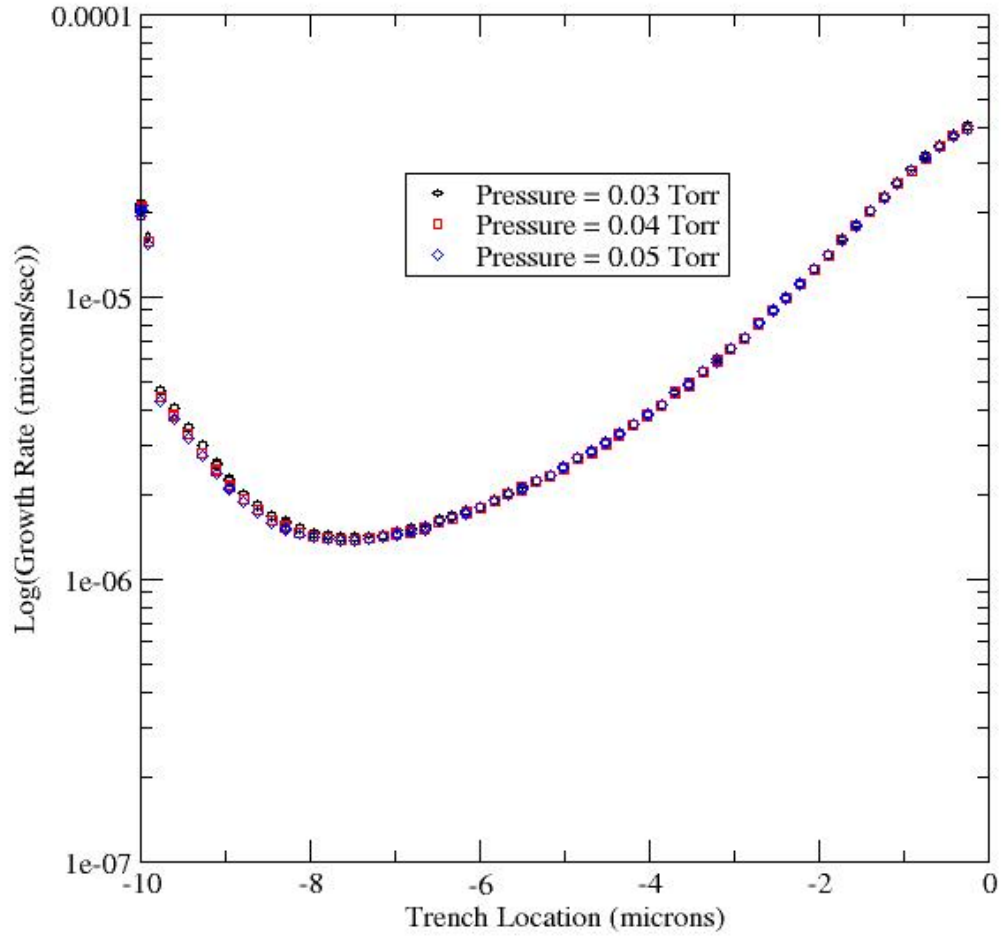


**Figure 5** Growth rates as a function of depth and reactor pressure of  $\text{SiO}_2$  in a PECVD process using  $\text{SiH}_4$  and  $\text{O}_2$ . The ion energy is 15 eV in each case.

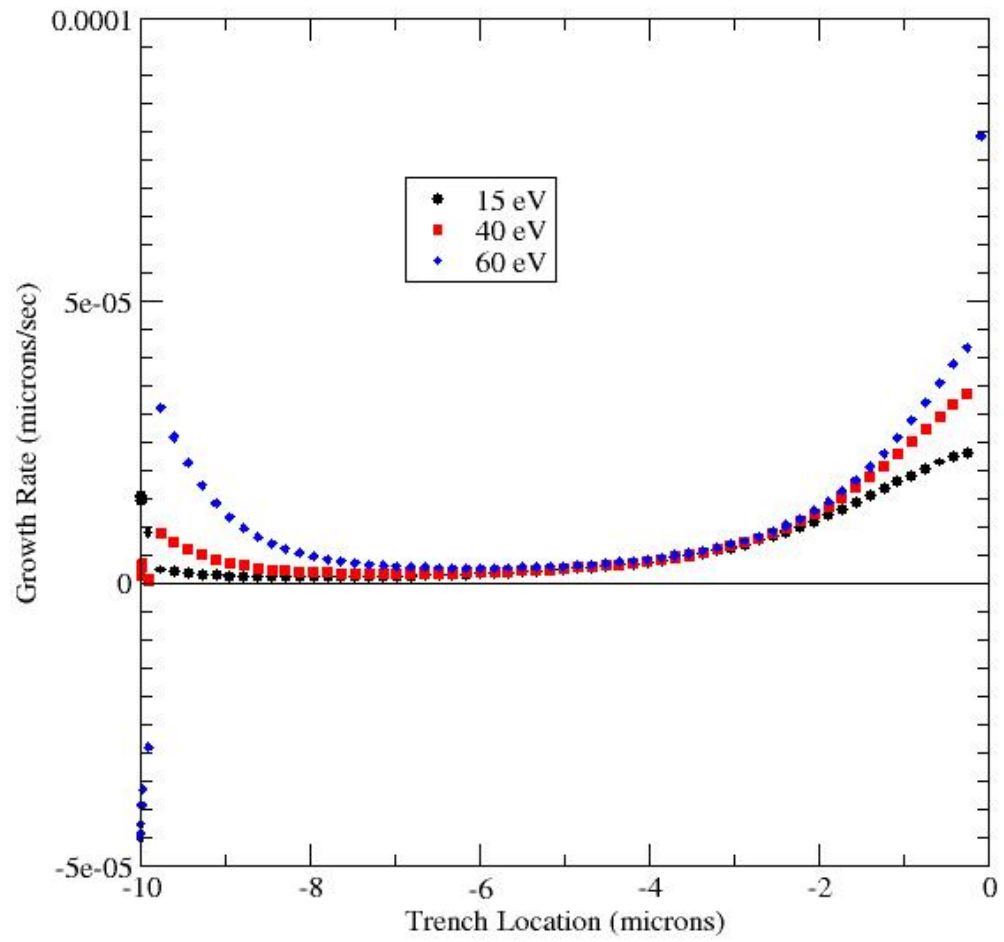


**Figure 6** Growth rates as a function of depth and ion energy of SiO<sub>2</sub> in a PECVD process using SiH<sub>4</sub> and O<sub>2</sub>. The reactor pressure is 0.03 Torr in each case.



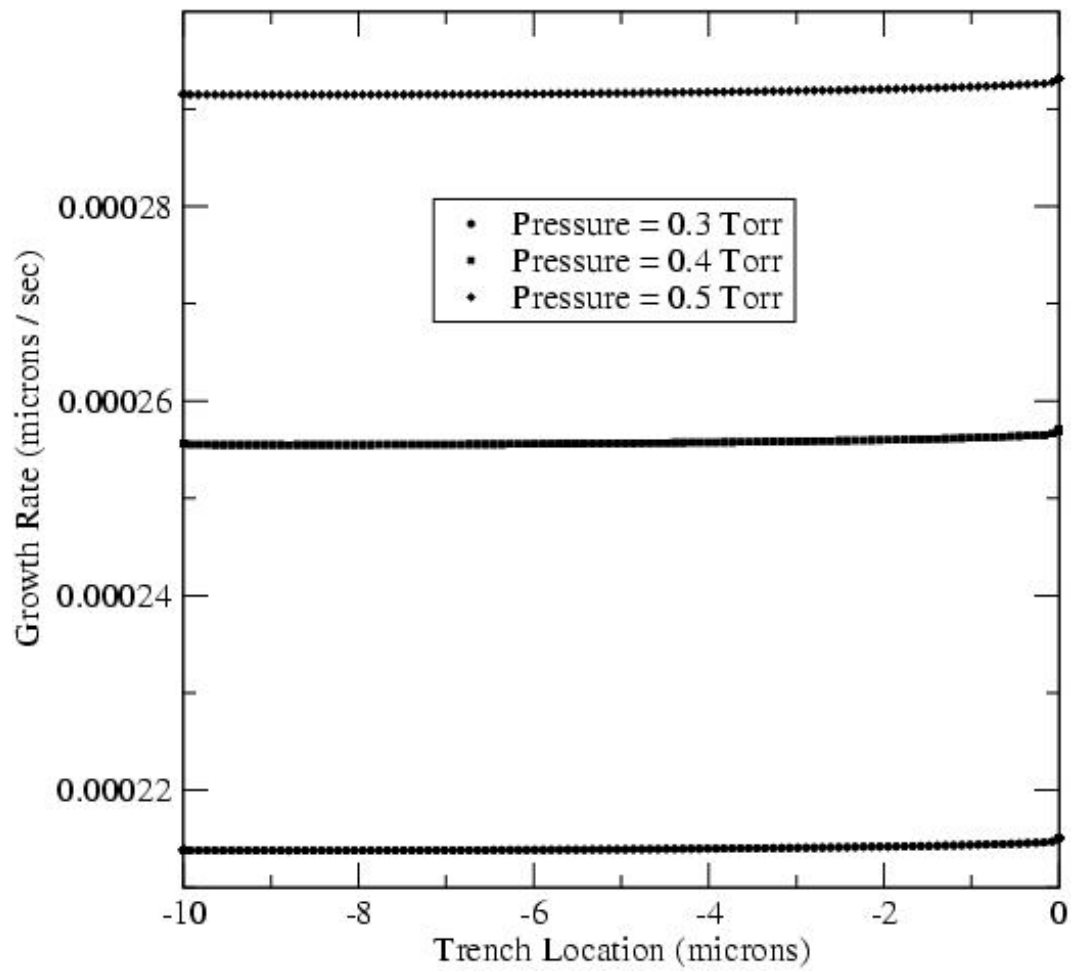


**Figure 7** Growth rate as a function of depth of SiO<sub>2</sub> in a LPCVD process using TEOS-- Coltrin's chemistry.

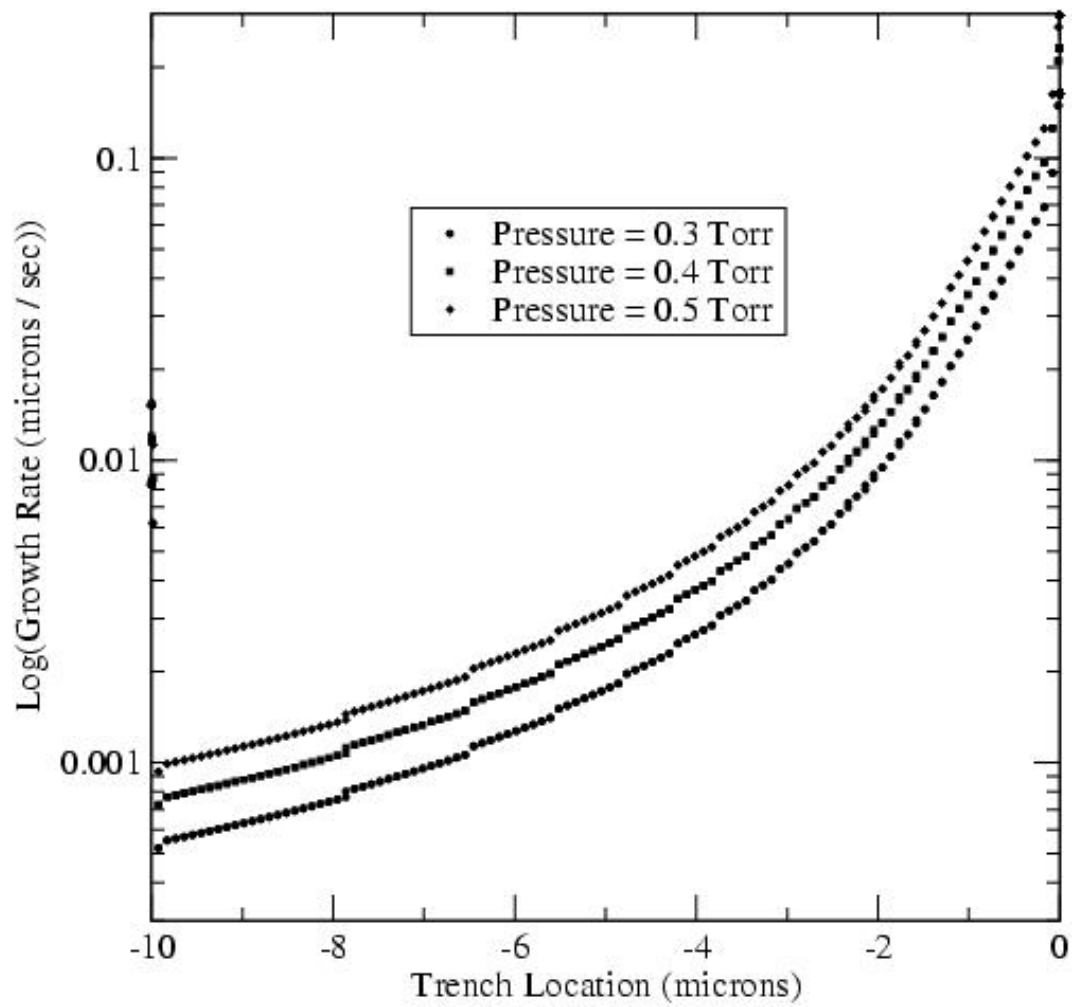


**Figure 8** Growth rate as a function of depth of SiO<sub>2</sub> in a LPCVD process using TEOS---IslamRaja's chemistry.